The Journal of Green Energy and Environmental Engineering

Research Paper

Preparation and Sensing Performance of Camellia Saponin-based Conductive Hydrogel

Samuel Morgan[1,*], Hannah Evans[2]

[1] Chemical and Environmental Engineering Department, University of Cambridge, Cambridge, UK
[2] St. Petersburg Federal Research Center of the Russian Academy of Sciences, St. Petersburg Institute for Informatics and Automation of the Russian Academy of Sciences, 14th line, 39, St. Petersburg 199178, Russia
*Corresponding author: scmorgan@cam.ac.uk; 0323evans@inbox.ru

Abstract. Eco-friendly, natural, biodegradable, and economical camellia saponin (S) was utilized as raw material to prepare a conductive hydrogel with excellent mechanical properties. First, camellia saponin was dissolved in a water/glycerol (G) mixture, followed by the addition of polyvinyl alcohol (PVA) and stirring at 105°C for 3 h. The solution was then subjected to freeze-thaw cycling at −20°C and 25°C to obtain polyvinyl alcohol-glycerol-camellia saponin (PGS) hydrogel. Subsequently, an iron chloride solution was added to undergo a metal chelation reaction, resulting in the formation of polyvinyl alcohol-glycerol-camellia saponin-ferric ion (PGSF) hydrogel consisting of polyvinyl alcohol, glycerol, camellia saponin, and Fe^{3+}. In parallel, neat PVA (P), PVA/glycerol (PG) and PVA/camellia-saponin (PS) hydrogels were fabricated as benchmarks to compare mechanical, electrical and sensing characteristics. Coordination between ferric ions and camellia saponin markedly boosted both the mechanical robustness and charge-transport ability of the network. The optimised hydrogel sustained an ultimate elongation of 1 038 % and a tensile strength of 1.28 MPa. Under cyclic loading—150 % tensile strain and 50 % compressive strain—it displayed minimal hysteresis, evidencing excellent elastic stability. Electrically, the material exhibited a conductivity of 1.99 S m^{-1} and a gauge factor of 2.48. When integrated into a flexible wearable sensor, it produced stable, reproducible relative-resistance profiles during flexion of the fingers, wrists, elbows and knees, demonstrating reliable real-time monitoring of human joint motion.

Keywords: *biobased materials; mechanical properties; sensor*

Received on 02 March 2026, Accepted on 05 June 2026, Published on 07 July 2026

1 Introduction

Hydrogels, built from water-loving three-dimensional polymer architectures [1], find extensive deployment across tissue engineering, pharmaceutical delivery, conformable sensing, wound care, soft electronics, and beyond [2–5]. Yet conventional hydrogel formulations are plagued by inadequate mechanical integrity, vulnerability to external stimuli, limited functional scope, and poor sustainability. Insufficient mechanical performance often limits their application scope as sensors. To address this, researchers have proposed strategies involving changes in crosslinking agents. Zhang et al. [6] used a novel crosslinker to improve the mechanical properties of hydrogels, achieving a tensile strength of 0.65 MPa, but this method involved many chemically synthesized substances that are harmful to the environment and human body, and the mechanical properties of the hydrogel still need further improvement. To solve this problem, Yan et al. [7] utilized carboxymethyl chitosan carboxyl groups to form coordination bonds with metal cations such as Fe^{3+}, preparing a high-strength hydrogel with a tensile strength exceeding 2 MPa. However, carboxymethyl chitosan is generally extracted from crustacean shells such as shrimp and crab, followed by chemical processing, resulting in low yield and complex preparation, which is not conducive to sustainable development. Therefore, it is necessary to develop a natural, degradable, and high-yield material to solve the above problems. Camellia saponin derived from oil-tea cake is a natural non-ionic surfactant, composed of sapogenin, sugar moiety, and organic acid,

accounting for about 15% of the mass of oil-tea cake [8]. Camellia saponin is mainly used as a pond cleaner for shrimp and crab farming and a concrete air-entraining agent, lacking deep processing and high-value utilization products. According to relevant research reports [9], camellia saponin molecules are rich in active functional groups such as carboxyl, carbonyl, and hydroxyl groups, which can coordinate with metal ions, achieving the effect of chelating metal ions similar to carboxymethyl chitosan. In addition, to extend the service life of hydrogels in harsh environments, glycerol is often introduced as a humectant and antifreeze agent [10]. Based on this, this study used green, natural, degradable, and economical camellia saponin as raw material, and prepared hydrogels by heating, freeze-thaw, introducing glycerol, and chelating Fe^{3+}. Multiple analytical methods were used to characterize the structure of the hydrogels, and the mechanical, conductive, and sensing properties were tested, aiming to provide a theoretical basis and technical reference for constructing sustainable conductive hydrogels with good mechanical properties.

2 Experimental

2.1 Materials, reagents and instruments

Camellia saponin (S, 70 % assay) was sourced from Jiangxi Xinzhongye Tea Technology. Polyvinyl alcohol (PVA) and glycerol (G) were procured from Aldrich Chemical Reagent. Ferric chloride ($FeCl_3$) was obtained from Macklin Biochemical. All chemicals were employed as received without additional purification. Instrumentation included a Nicolet iS50 FT-IR spectrometer (Thermo Fisher Scientific, USA), a Zeiss Sigma 300 field-emission SEM equipped with an EDS detector (Germany), and a Bruker D8 XRD system (Bruker, USA). UV-2550 ultraviolet-visible spectrophotometer, Shimadzu, Japan; STA 2500 thermogravimetric (TG) analyzer, Netzsch, Germany; UTM 2503 electronic universal testing machine, Shenzhen Sansi Zongheng Technology Co., Ltd.; CHI 760E electrochemical workstation, Cichadou Co., Ltd.; TH 2830 impedance analyzer, Tonghui Electronic Co., Ltd.

2.2 Preparation of hydrogels

Initially, 5 g of camellia saponin (S) and 10 g of polyvinyl alcohol (PVA) were dispersed into 100 g of an aqueous glycerol medium prepared at a 1:1 mass ratio. The blend was mechanically agitated at 105 °C for 3 h to obtain a homogeneous solution, which was subsequently cast into a 60 mm × 60 mm × 20 mm mould. After a 12 h reaction at −20 °C, the gel was equilibrated at 25 °C for 2 h to yield the polyvinyl alcohol–glycerol–camellia saponin (PGS) hydrogel. Finally, the prepared PGS hydrogel was immersed in 50 g of 30 wt% $FeCl_3$ solution at room temperature, taken out after 20 min, and wiped dry with filter paper to obtain PGSF hydrogel. For comparison, P, PG, and PS hydrogels were prepared. Among them, P is polyvinyl alcohol hydrogel, prepared by heating and freeze-thawing PVA (10 g) and water (50 g); PG is polyvinyl alcohol/glycerol hydrogel, prepared by heating and freeze-thawing PVA (10 g) and water/glycerol solution (100 g); PS is polyvinyl alcohol/camellia saponin hydrogel, prepared by heating and freeze-thawing PVA (10 g), camellia saponin (5 g), and water (50 g). The temperature and time of heating and freeze-thawing for all hydrogels were the same.

2.3 Testing and characterization of hydrogels

2.3.1 Structural characterization

FT-IR instrument was used to test dry hydrogel samples in the range of 400–4 000 cm^{-1}; SEM and EDS were used to observe the microstructure of hydrogel samples; X-ray diffraction patterns were recorded on a powder diffractometer equipped with a Cu Kα source (λ = 0.15418 nm), scanning from 5° to 90° (2θ) at 5° min^{-1}. Thermogravimetric analysis of the hydrogels was performed under a helium atmosphere over the temperature range 25–800 °C, applying a heating ramp of 20 °C min^{-1}. The optical transmittance spectra of the hydrogels across the 400–800 nm wavelength window were further acquired on a UV–visible spectrophotometer.

2.3.2 Mechanical property test

Electronic universal testing machine was used to test the mechanical properties of hydrogels. Tensile test: hydrogel was cut into dumbbell-shaped specimens of 1.6 mm × 27 mm × 4 mm, tensile speed 100 mm/min, each sample was tested 3 times and averaged. Compression test: hydrogel was cut into cylinders of ϕ22 mm × 16 mm,

using a 200 N load sensor, compression speed 5 mm/min, each sample was tested 3 times and averaged. Tensile stress (ω) and tensile strain (ε) were calculated by equations (1) and (2):

$$\omega = F / A_o$$

$$\varepsilon = (L_1 - L_o) / L_o$$

where ω is tensile stress (MPa); ε is tensile strain (%); F is applied load (N); A_o is the cross-sectional area of the original specimen (m^2); L_1 is the length after stretching (m); L_o is the original length (m).

2.3.3 Conductive property test

CHI 760E electrochemical workstation was used for measurement. Conductivity was calculated by equation (3):

$$\sigma = L / (R\_b \times A)$$

where σ is conductivity (S/m); R_b is the resistance of the specimen (Ω); L is the length of the specimen (m); A is the cross-sectional area of the specimen (m^2).

2.3.4 Sensing property test

The hydrogel sample was connected to an LCR digital bridge through copper wires and tested with the assistance of an electronic universal testing machine. Relative resistance change rate ($\Delta R/R_o$) and sensitivity (G_F) were calculated by equations (4) and (5):

$$\Delta R/R_o = (R - R_o) / R_o \times 100\%$$

$$G\_F = (R - R_o) / (R_o \times \varepsilon')$$

where ΔR is the resistance change value of the hydrogel during stretching (Ω); R_o is the initial resistance (Ω); R is the real-time resistance of the hydrogel under a certain deformation (Ω); G_F is the sensitivity of the strain sensor; ε' is the strain of the hydrogel when testing sensing properties (%).

3 Results and Discussion

3.1 Structural characterization of hydrogels

3.1.1 Morphology analysis

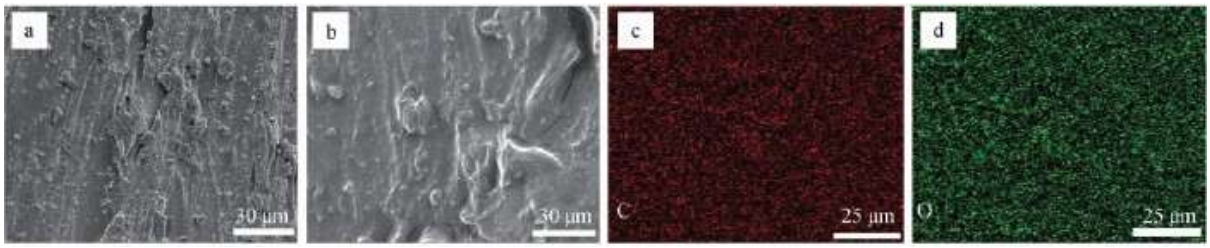

Figure 1 SEM (a–b) and EDS (c–d) analysis of hydrogels

SEM was used to study the cross-sectional microstructure of hydrogels. Compared with the SEM image of pure polyvinyl alcohol hydrogel P (Fig. 1(a)), hydrogel PS (Fig. 1(b)) had a relatively dense structure. This is because camellia saponin molecules and polyvinyl alcohol molecules are tightly bound together through van der Waals forces. The EDS analysis results in Fig. 1(c) and (d) show that C and O elements are evenly distributed on the surface of the hydrogel.

3.1.2 FT-IR analysis

FT-IR spectroscopy verified the effective incorporation of camellia saponin as well as the coordination interaction between ferric ions and the saponin moieties. The spectra presented in Fig. 2(a) compare camellia saponin, the PGS hydrogel, and the PGSF complex. The broad band at 3320 cm^{-1} corresponds to O–H stretching vibrations within the saponin structure, whereas the peak at 1600 cm^{-1} is ascribed to the carbonyl functionality characteristic of camellia saponin [11]. A comparison between PGS and PGSF reveals noticeable shifts in the absorption maxima: the bands originally located near 1650 and 3320 cm^{-1} in PGS migrate to 1640 and 3280 cm^{-1}, respectively, in PGSF. Such spectral displacements signify structural alterations within the hydrogel matrix, confirming that Fe^{3+} establishes coordinate bonds with active functional groups including hydroxyl and carbonyl moieties [12].

3.1.3 XRD analysis

Fig. 2(b) shows the XRD test results of hydrogels. It can be seen that the characteristic diffraction peak of camellia saponin is at 13.72°, while the diffraction peak intensities of PGS and PGSF at 13.72°, 19.4°, and 40.32° are lower than those of PG, because camellia saponin and Fe^{3+} affected the formation of PVA crystals [13].

3.1.4 Thermogravimetric analysis

Thermogravimetric characterisation was employed to appraise the thermal robustness of the hydrogel networks. The TG profiles displayed in Fig. 2(c) trace the mass-loss behaviour of lyophilised specimens heated from 25 °C to 800 °C. Throughout this temperature window, both PGS and PGSF formulations demonstrated markedly superior weight retention relative to the P and PG counterparts. The pronounced thermal resilience inherent to camellia saponin, evident from its thermogravimetric trace, is instrumental in bolstering the overall thermal stability of the composite hydrogels.

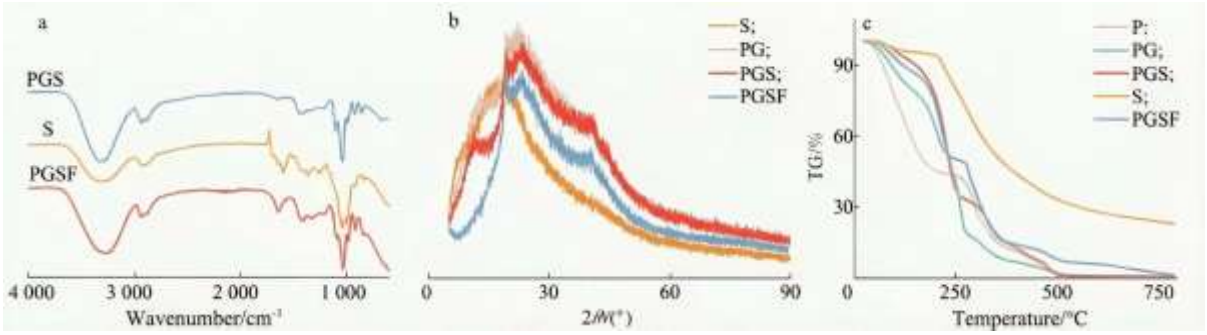

Figure 2 FT-IR spectra (a), XRD curves (b) and TG (c) of hydrogels

3.1.5 Transmittance test

The transmittance of hydrogels at room temperature (25°C) was measured by transmission spectroscopy. Fig. 3(a) shows that the freeze-thaw treated hydrogel PGS has high transparency; from Fig. 3(b), it can be seen that the transmittance of freeze-thaw treated hydrogel PGS at 750 nm reaches 83%, while the control group without freeze-thaw treatment has poor transmittance, only 15%, indicating that freeze-thaw treatment can improve the transparency of hydrogels. In addition, as shown in Fig. 3(c), with the increase of camellia saponin dosage, the transmittance of hydrogels decreases.

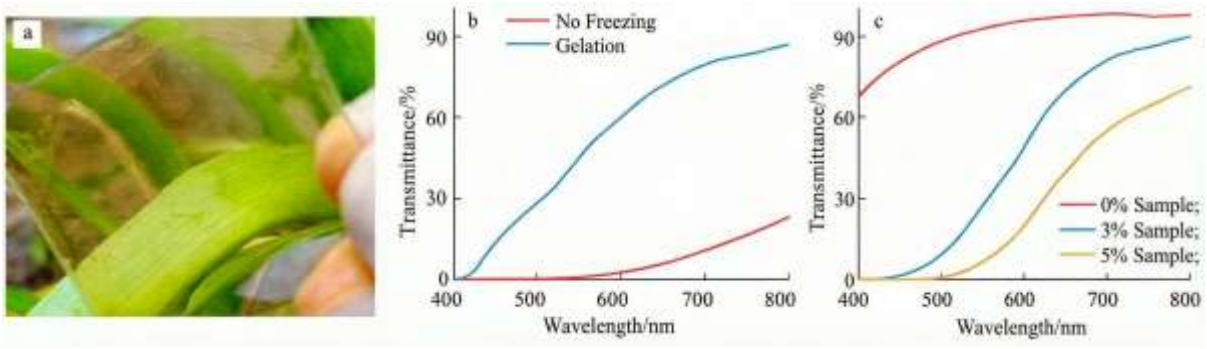

Figure 3 Image (a) and transmittance (b–c) of PGS hydrogel

3.2 Mechanical properties of PGSF hydrogel

Prolonged functionality necessitates that hydrogels retain sufficient ductility and tenacity. The mechanical profile of PGSF was therefore rigorously evaluated. Photographic evidence in Fig. 4 demonstrates that, whether pristine, twisted, or knotted, the hydrogel undergoes facile elongation (Fig. 4a) and sustains compressive and tensile loads exerted by a 0.5 kg object (Fig. 4b), confirming its superior toughness and elastic behaviour.

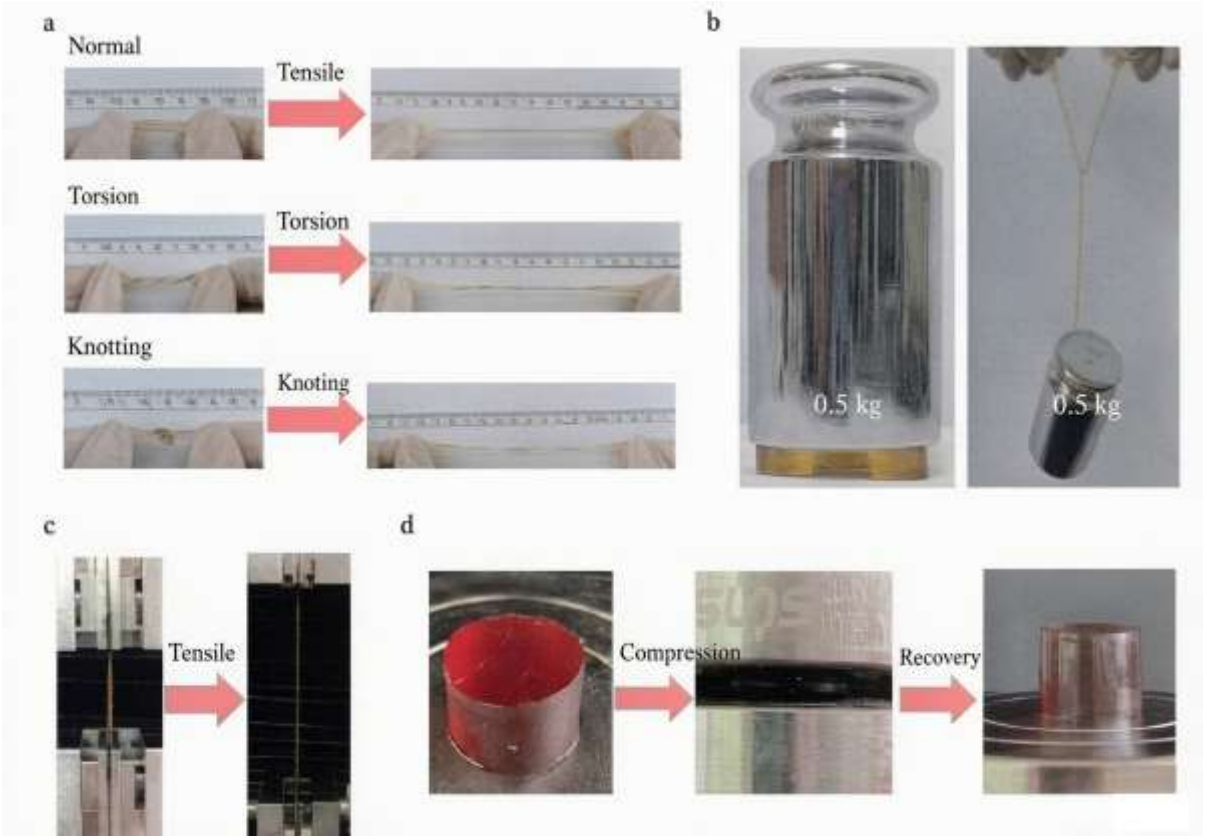

Figure 4 Images of PGSF hydrogels under various external forces

Subsequently, tensile stress-strain tests were performed on PGSF hydrogel. Fig. 4(c) shows the image of tensile testing of hydrogels by universal testing machine. The hydrogel was continuously stretched until fracture, and then the stress and strain values at fracture were recorded. In addition, in the compression test image of Fig.

4(d), PGSF hydrogel can still recover after being compressed to 50% strain, proving that it has good compression cycle stability.

Figure 5a illustrates how camellia saponin loading influences the mechanical response. As the saponin content rose from 0 to 5 wt%, both the ultimate tensile strength and the elongation at break registered modest gains, with the latter climbing from 616 % to 683 % and the former increasing from 1.05 MPa to 1.20 MPa. The impact of freeze–thaw cycling on the stress–strain behaviour is depicted in Figure 5b. A single freeze–thaw cycle dramatically boosted the elongation at break from 446 % to 683 % and the tensile strength from 0.20 MPa to 1.20 MPa. This pronounced enhancement stems from the formation of crystalline microdomains within the PVA matrix during freezing, which fosters physical cross-linking among polymer chains and elevates the network density [14]. Yet, further cycling proved detrimental: after two and three cycles, the tensile strength receded to 0.68 MPa and 0.71 MPa, respectively. The role of Fe^{3+} coordination is examined in Figure 5c. Chelation of ferric ions with the PGS hydrogel markedly amplified its mechanical performance, extending the elongation at break from 682 % to 1 038 % while raising the tensile strength from 1.19 MPa to 1.28 MPa. This improvement is attributed to the reversible dissociation of ionic coordination bonds formed between the carboxyl functionalities of camellia saponin and Fe^{3+} during deformation; these sacrificial bonds fracture and reform to dissipate mechanical energy, thereby fortifying the hydrogel [15].

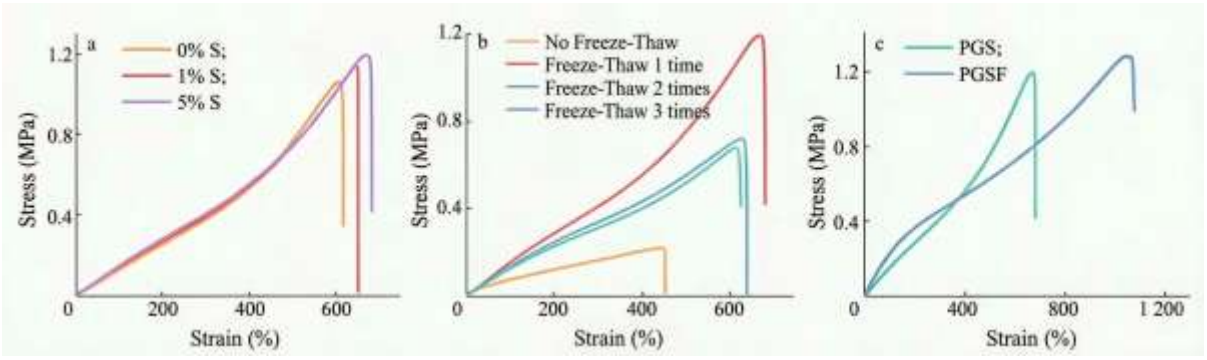

Figure 5 Effect of different preparation conditions on the tensile properties of the PGSF hydrogels

The mechanical behaviour of the hydrogels was further interrogated through uniaxial compression assays. Figure 6a presents the compressive stress–strain trace of the PGSF formulation. In contrast to the inherent brittleness typical of conventional hydrogels, this specimen displayed pronounced toughness, withstanding compressive stresses in excess of 9 MPa. Because long-term deployment demands both durability and recyclability, the PGSF hydrogel was subjected to successive tensile and compressive cycling protocols to ascertain whether its mechanical integrity is preserved under repeated deformation.

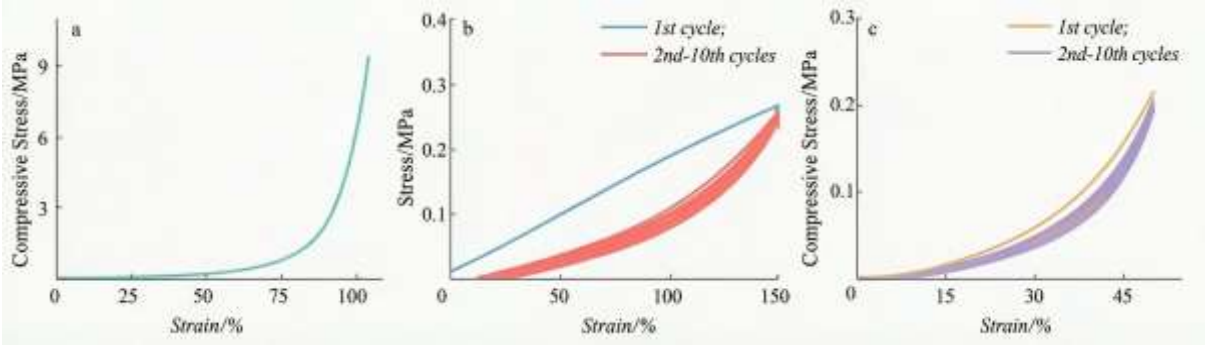

Figure 6 Stress-strain curves of compression (a), cyclic tension (b) and cyclic compression (c) of PGSF hydrogels

As shown in Fig. 6(b), when the hydrogel was stretched to 150% strain for 10 cycles, the curve area of the first cycle was large, indicating that a large amount of energy was dissipated in the first cycle; in the 2nd to 10th

cycles, the curves almost overlapped, indicating that the hysteresis curve of the hydrogel was small. In contrast, the cyclic compression stability of PGSF hydrogel was higher. As illustrated in Fig. 6(c), the PGSF hydrogel underwent ten successive compression cycles at 50 % strain. The initial cycle displayed a marginally larger hysteresis area than the subsequent nine, which all exhibited consistently compact loop profiles. These characteristics prove that the hydrogel has good stability and recovery, providing necessary conditions for hydrogels as flexible sensors [16].

3.3 Conductive and sensing properties of PGSF hydrogel

Conductive property is one of the important conditions for hydrogels as flexible sensor applications [17]. With the increase of camellia saponin dosage (1%–10%), the conductivity of PGS hydrogel was only 0.02 S/m at most. As can be seen from Fig. 7(a), the conductivity of hydrogels increased significantly after chelating metal Fe^{3+}, and when the camellia saponin dosage was 10%, the conductivity reached 1.99 S/m at most. From Fig. 7(b), it can be seen that after adding ferric ions to PGS hydrogel, the LED bulb became brighter. Compared with the conductive properties of other biomass conductive hydrogels (such as starch-based ionic conductive hydrogel with a conductivity of 0.96 S/m [18]), this hydrogel has good conductive properties.

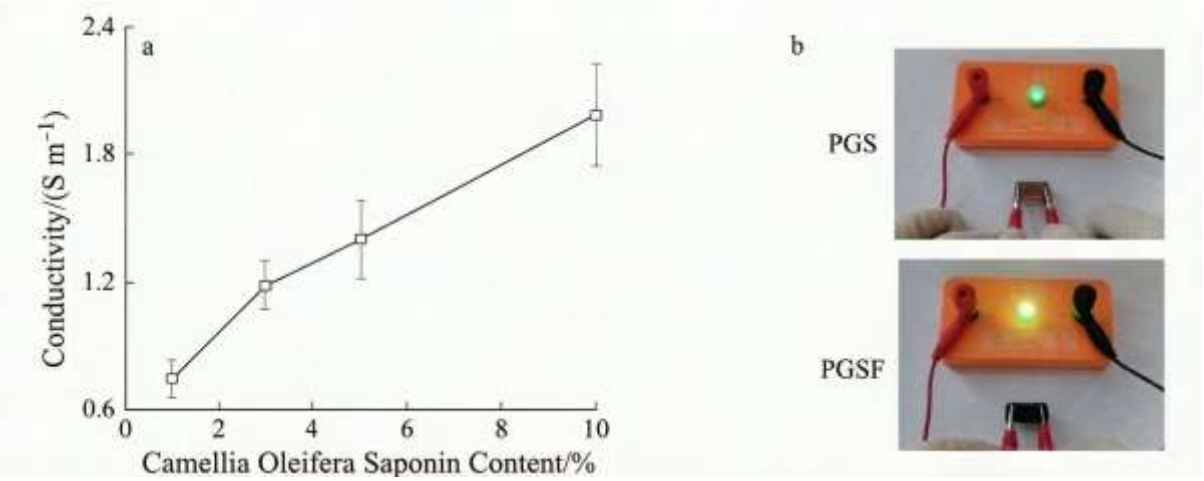

Figure 7 Conductive properties tests of PGSF hydrogels

Figure 8a demonstrates that the hydrogel's relative resistance exhibits a systematic, reproducible dependence on applied strain with modest fluctuation amplitude. The gauge factor (G_F), defined as the slope of the relative resistance change versus strain plot (Fig. 8b), characterises the sensor's electromechanical sensitivity. Linear regression of the strain–resistance response yields G_F values of 1.23 (R^2 = 0.99) within 0–100 % strain and 2.48 (R^2 = 0.99) over the 100–400 % strain interval, confirming the material's excellent signal-transduction capability as a flexible sensor. The durability of hydrogels is an important factor in evaluating their potential as strain sensors. Over 100 loading–unloading cycles spanning 0–100 % tensile strain (Fig. 8c), the resistance signal remained notably stable, ensuring the hydrogel avoids failure during prolonged cyclic motion.

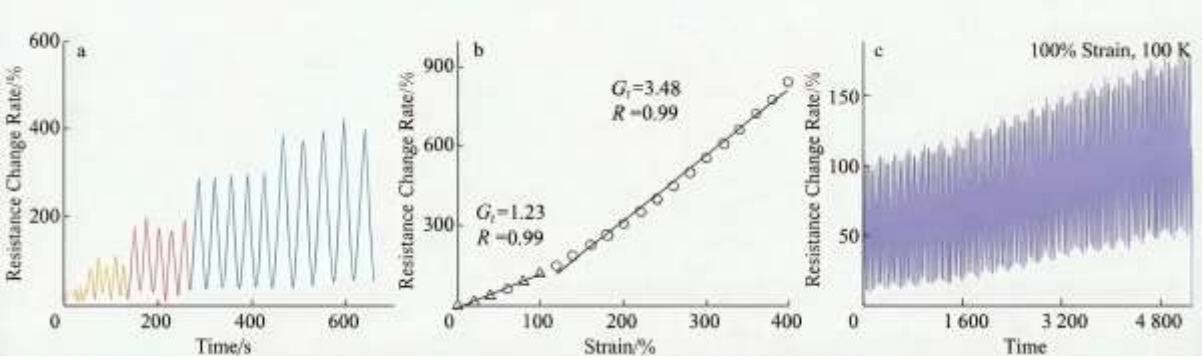

Figure 8 Strain sensing performance tests of hydrogels

3.4 Sensing applications of PGSF hydrogel

The PGSF hydrogel demonstrates robust strain-sensing characteristics, making it well suited for deployment as a compliant strain transducer. To validate its practical utility, the material was fabricated into a wearable sensor and affixed to various human joints to capture motion-induced deformation. As depicted in Fig. 9, the electrical output recorded during repeated finger flexion–extension cycles proved highly reproducible and stable, attesting to the sensor's reliable sensitivity and operational durability. Distinct articulatory motions impose different degrees of elongation on the hydrogel film, which in turn modulates its relative resistance in a motion-specific manner. Consequently, by examining the morphological features of the signal traces—including peak shape, pulse width, and amplitude—different joint kinematic patterns can be unambiguously discriminated. For instance, a 90° finger flexion elicited a maximal relative resistance change of approximately 80 %, whereas increasing the bend angle to 120 % drove the peak response to roughly 100 %. Therefore, the flexible sensor based on PGSF hydrogel can stably, quickly, and accurately detect various human movements.

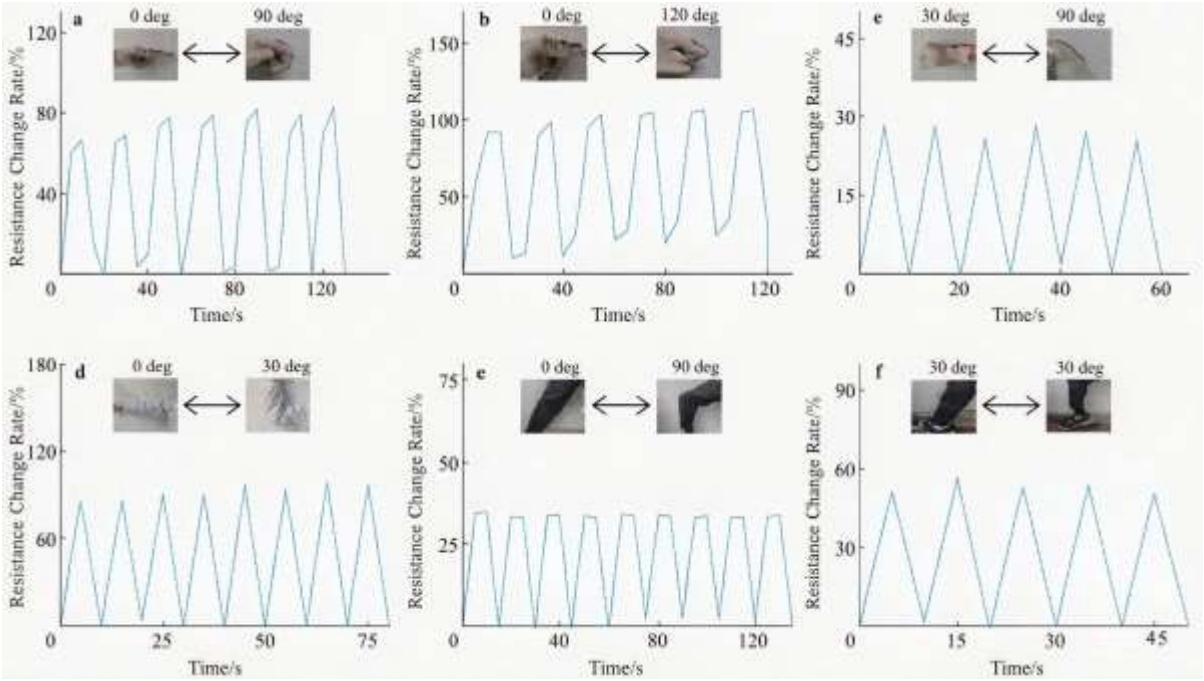

Figure 9 Application tests of sensing performance of hydrogels

Based on the structural characterization and performance data presented above, the working mechanism of the camellia saponin-based conductive hydrogel (PGSF) can be elucidated through a multi-level analysis of molecular interactions, energy dissipation, ion transport, and strain-responsive electrical signaling. The entire mechanism is rooted in the synergistic integration of a biopolymer network, a natural surfactant, and dynamic metal coordination chemistry.

The primary scaffold is formed by polyvinyl alcohol (PVA) chains that undergo freeze-thaw cycling at −20°C and 25°C. During freezing, ice crystals act as porogens and templates, expelling PVA chains into the interstitial spaces where they aggregate into crystalline microdomains. These microdomains serve as physical crosslinking nodes, significantly enhancing the hydrogel's mechanical integrity. The introduction of glycerol, a biocompatible humectant, not only prevents excessive ice crystal growth but also forms strong hydrogen bonds with PVA hydroxyl groups, maintaining flexibility and imparting anti-drying and anti-freezing properties. This physical network provides the foundational toughness and elasticity observed in the PGS hydrogel.

Camellia saponin (S), a natural triterpenoid saponin extracted from oil-tea cake, is rich in carboxyl, carbonyl, and hydroxyl groups. When blended into the PVA/glycerol system, saponin molecules intercalate within the polymer

matrix and establish extensive van der Waals forces and hydrogen bonds with PVA chains. This intermolecular entanglement creates a denser, more compact microstructure, as evidenced by SEM images showing a tighter cross-section in PS hydrogels compared to pure PVA. The saponin molecules essentially act as molecular "rivets," reinforcing the network and contributing to a moderate increase in tensile strength (from 1.05 to 1.20 MPa) and elongation at break (from 616% to 683%).

The most critical enhancement arises from the chelation of Fe^{3+} ions with camellia saponin. The carboxyl and carbonyl groups of saponin serve as multidentate ligands that coordinate with Fe^{3+} to form reversible ionic crosslinks. This transforms the physically crosslinked network into a dual-network system combining covalent-like physical junctions (crystalline domains) and dynamic coordination bonds. During mechanical deformation, these Fe^{3+}-saponin coordination bonds function as sacrificial bonds: when tensile stress is applied, the weaker coordination bonds break preferentially before the polymer backbone fractures, dissipating energy and preventing catastrophic failure. Subsequently, the bonds can reform, enabling self-recovery. This mechanism explains the remarkable improvement in mechanical properties after $FeCl_3$ treatment—elongation at break surges to 1 038% and tensile strength to 1.28 MPa. The small hysteresis loops observed in cyclic tensile (150% strain) and compressive (50% strain) tests directly confirm efficient energy dissipation and excellent elastic recovery.

The same Fe^{3+}-saponin coordination chemistry underpins the hydrogel's electrical conductivity. Before metal incorporation, the PGS hydrogel exhibits negligible conductivity (≤0.02 S/m) because charge carriers are scarce. Upon immersion in $FeCl_3$ solution, Fe^{3+} ions diffuse into the network and coordinate with saponin ligands. These bound ions, along with residual free Cl^- and Fe^{3+} in the glycerol-water solvent, create an ionic conduction pathway. The glycerol-water binary solvent facilitates ion mobility by maintaining a fluid, non-frozen liquid phase even at sub-zero temperatures. Consequently, conductivity jumps to 1.99 S/m—surpassing many biomass-based conductive hydrogels (e.g., starch/ionic liquid hydrogels at 0.96 S/m). The LED brightness test visually corroborates this enhancement.

The PGSF hydrogel operates as a resistive strain sensor based on deformation-induced changes in ion transport efficiency. In the resting state, the hydrogel possesses a baseline resistance R_0 determined by the fixed distance between electrodes and the intrinsic conductivity. When stretched, two coupled effects occur: (1) geometric elongation increases the distance between conductive ions, raising the effective resistance; (2) narrowing of the hydrogel cross-section reduces the ion transport channel area, further impeding current flow. These changes produce a relative resistance change $\Delta R/R_0$ that scales with applied strain. The gauge factor (GF) is not constant but strain-dependent: in the low-strain regime (0–100%), GF = 1.23, reflecting primarily elastic deformation with reversible bond stretching; in the high-strain regime (100–400%), GF rises to 2.48, indicating the involvement of microcrack formation and greater alignment of polymer chains that exponentially increases resistance. The linear fitting (R^2 = 0.99) in both regions demonstrates predictable, reproducible sensing behavior.

When assembled into a flexible sensor, the PGSF hydrogel adheres conformally to skin. Joint bending (fingers, wrists, elbows, knees) induces tensile strain on the hydrogel, generating characteristic resistance peaks. The amplitude of $\Delta R/R_0$ correlates with bending angle—e.g., 80% at 90° finger flexion and 100% at 120°—allowing precise differentiation of movement intensity. The stability over 100 cyclic loading-unloading tests confirms that the dynamic coordination bonds and physical crosslinks withstand repeated deformation without permanent damage, making the sensor reliable for long-term health monitoring.

In summary, the PGSF hydrogel's exceptional performance originates from a hierarchical design: PVA crystalline domains provide structural backbone, glycerol ensures environmental resilience, camellia saponin reinforces the matrix via hydrogen bonding, and Fe^{3+} coordination introduces dynamic sacrificial bonds for toughness and ionic conductivity. This multifunctional synergy translates into a material that is mechanically robust, electrically conductive, and highly sensitive—ideal for flexible wearable electronics and human motion detection.

4 Conclusions

Camellia saponin is a natural compound, and preparing hydrogels from it as raw material is a new way to effectively utilize forest resources. The integration of freeze–thaw cycling with ferric-ion chelation

simultaneously reinforces the mechanical integrity, electrical conductivity, and sensory responsiveness of the resulting hydrogels. Assembled into a compliant strain sensor, the camellia saponin-derived hydrogel reliably deciphers human body motions, underscoring its viability as a stretchable sensing platform. Consequently, this material holds considerable promise for wearable sensing technologies, while also broadening the utilisation of forest-derived biomass and advancing the sustainable evolution of hydrogel systems.

References

[1] GUO Y H, BAE J, FANG Z W, et al. Hydrogels and hydrogel-derived materials for energy and water sustaina bility[J]. Chemical Reviews, 2020, 120(15): 7642–7707.

[2] WANG X M, WENG L, ZHANG X R, et al. Constructing conductive and mechanical strength self-healing hyd rogel for flexible sensor[J/OL]. Journal of Science: Advanced Materials and Devices, 2023, 8(3): 100563[20 23-12-25]. https://doi.org/10.1016/j.jsamd.2023.100563.

[3] TAN L, LI M H, CHEN H, et al. Dynamic hydrogel with environment-adaptive autonomous wound-compres sing ability enables rapid hemostasis and inflammation amelioration for hemorrhagic wound healing[J/O L]. Nano Today, 2023, 52: 101962[2023-12-25]. http://doi.org/10.1016/j.nantod.2023.101962.

[4] LI M, GUAN Q W, LI C, et al. Self-powered hydrogel sensors[J/OL]. Device, 2023, 1(1): 100007[2023-12-25]. 10.1016/j.device.2023.100007.

[5] LI B A, CHEN Y R, WU W, et al. Copolymer-grafted cellulose nanocrystal induced nanocomposite hydrogels with enhanced strength, high elasticity and adhesiveness for flexible strain and pressure sensors[J/OL]. C arbohydrate Polymers, 2023, 317: 121092[2023-12-25]. https://doi.org/10.1016/j.carbpol.2023.121092.

[6] ZHANG D, LIU Y L, GROSS W, et al. Designing antifreezing hydrogels with enhanced mechanical properties using a simple crosslinker[J/OL]. Giant, 2023, 16: 100203[2023-12-25]. https://doi.org/10.1016/j.giant.20 23.100203.

[7] YAN K, WAN Y K, XU F Y, et al. Ionic crosslinking of alginate/carboxymethyl chitosan fluorescent hydrogel f or bacterial detection and sterilization[J/OL]. Carbohydrate Polymers, 2023, 302: 120427[2023-12-25]. htt ps://doi.org/10.1016/j.carbpol.2022.120427.

[8] LEE J, LIM J H, JUNG G Y, et al. Triterpenoid saponins from Camellia sinensis roots with cytotoxic and imm unomodulatory effects[J/OL]. Phytochemistry, 2023, 212: 113688[2023-12-25]. https://doi.org/10.1016/j. phytochem.2023.113688.

[9] HU J H, CHEN X X. The review of the chemical structure, physical and chemical properties on the tea sapo nin, tea polysaccharide and saccharicterpenin[J]. Journal of Wuhan Polytechnic University, 2012, 31(2): 20 –23.

[10] HU C X, ZHANG Y L, WANG X D, et al. Stable, strain-sensitive conductive hydrogel with antifreezing capabil ity, remoldability, and reusability[J]. ACS Applied Materials & Interfaces, 2018, 10(50): 44000–44010.

[11] GAO Z B, YE M, XUE L L, et al. Extraction technology study of tea saponin from oil-tea-cakes by supersonic -ethanol method[J]. Chemical Engineering & Equipment, 2018(2): 41–46.

[12] KANG M M, ODERINDE O, LIU S L, et al. Characterization of Xanthan gum-based hydrogel with Fe^{3+} ions co ordination and its reversible sol-gel conversion[J]. Carbohydrate Polymers, 2019, 203: 139–147.

[13] CHEN Y N, PENG L F, LIU T Q, et al. Poly(vinyl alcohol)-tannic acid hydrogels with excellent mechanical pro perties and shape memory behaviors[J]. ACS Applied Materials & Interfaces, 2016, 8(40): 27199–27206.

[14] OU K K, DONG X, QIN C L, et al. Properties and toughening mechanisms of PVA/PAM double-network hydr ogels prepared by freeze-thawing and anneal-swelling[J]. Materials Science and Engineering: C, 2017, 77: 1017–1026.

[15] DU J Y, WANG X X, SONG R Y, et al. Application of adhesive controllable galactomannan hydrogel initiated by aluminum ions at room temperature in flexible sensors[J/OL]. Reactive and Functional Polymers, 2023, 193: 105738[2023-12-25]. https://doi.org/10.1016/j.reactfunctpolym.2023.105738.

[16] YANG J, KANG Q, ZHANG B, et al. Robust, fatigue resistant, self-healing and antifreeze ionic conductive su pramolecular hydrogels for wearable flexible sensors[J]. Journal of Industrial and Engineering Chemistry, 2022, 115: 162–170.

[17] ZENG Q, WAN S H, YANG S J, et al. Super stretchability, strong adhesion, flexible sensor based on Fe^{3+} dyn amic coordination sodium alginate/polyacrylamide dual-network hydrogel[J/OL]. Colloids and Surfaces A: Physicochemical and Engineering Aspects, 2022, 652: 129733[2023-12-25]. https://doi.org/10.1016/j.cols urfa.2022.129733.

[18] XU Q Y, HOU M H, WANG L F, et al. Anti-bacterial, anti-freezing starch/ionic liquid/PVA ion-conductive hydrogel with high performance for multi-stimulation sensitive responsive sensors[J/OL]. Chemical Engineering Journal, 2023, 477: 147065[2023-12-25]. https://doi.org/10.1016/j.cej.2023.147065.